International Journal of Pharmaceutics 624 (2022) 122028

Contents lists available at ScienceDirect

International Journal of Pharmaceutics

journal homepage: www.elsevier.com/locate/ijpharm

Improved ocular delivery of quercetin and resveratrol: A comparative study between binary and ternary cyclodextrin complexes

Luna Krstić [a], Pekka Jarho [b], Marika Ruponen [b], Arto Urtti [b,c], María J. González-García [a,d,*], Yolanda Diebold [a,d]

[a] Instituto de Oftalmobiología Aplicada (IOBA), Universidad de Valladolid, 47011 Valladolid, Spain
[b] School of Pharmacy, Faculty of Health Sciences, University of Eastern Finland, Yliopistonranta 1, 70210 Kuopio, Finland
[c] Drug Research Program, Division of Pharmaceutical Biosciences, Faculty of Pharmacy, University of Helsinki, Viikinkaari 5 E, 00014 Helsinki, Finland
[d] Centro de Investigación Biomédica en Red Bioingeniería, Biomateriales y Nanomedicina (CIBER-BBN), Instituto de Salud Carlos III, 28029 Madrid, Spain

ARTICLE INFO

Keywords:
Cyclodextrins
Dry eye disease
Hyaluronic acid
Ocular drug delivery
Quercetin
Resveratrol

ABSTRACT

The number of patients affected by Dry Eye Disease (DED) had notably increased worldwide, addressing the need of novel therapeutic approaches. Polyphenols, quercetin (QUE) and resveratrol (RSV) show necessary antioxidant and anti-inflammatory properties to manage DED, but their application as topical eyedrops is restricted by low aqueous solubility and low chemical stability. Cyclodextrins (CD) are widely used to improve physicochemical characteristics of drugs. Consequently, the aim of this study was to make a comparison between binary complexes with quercetin, resveratrol and cyclodextrins and tertiary complexes adding hyaluronic acid (HA). Both complexes were able to enhance solubility and stability of QUE and RSV. AFM imaging and DLS measurements disclose the formation of spherical nanoaggregates within tertiary complexes of both QUE and RSV with mean diameters of 103 and 82 nm. Neither complex demonstrated cytotoxic effect in *in vitro* studies in corneal (HCE) and conjunctival (IM-ConjEpi) cell lines. In HCE cells, complexes containing QUE or RSV at their highest concentrations were able to scavenge more than 95 % of the ROS that were produced intracellularly ($p < 0.005$). Similar response was observed with IM-ConjEpi cells. The antioxidant effect was maintained in the complexes with HA. This confirmed their potential as viable topical treatment for DED.

1. Introduction

Reactive oxygen species (ROS) play an important role in processes involving metabolic reactions or cell differentiation (Batliwala et al., 2017; Yang and Lian, 2020). However, when a disequilibrium between the production and the elimination of ROS takes place, oxidative stress is generated. This situation is often a result of a compromised antioxidant system (Nita and Grzybowski, 2016). The stress contributing ROS are often generated by exogenous sources like UV light, chemicals, and smoke. Unrestricted oxidative stress leads to damage of deoxyribonucleic acid (DNA), proteins or lipids, and emergence of pathological states and inflammation (Cabrera and Chihuailaf, 2011; (Batliwala et al., 2017).

The direct contact of the anterior surface of the eye with the external environment makes it susceptible to oxidative stress. The structures of the ocular surface (cornea, conjunctiva, tear film, lacrimal and Meibomian glands) represent the first line of ocular protection against oxidative damage (Vizzarri et al., 2018). It is known that oxidative stress and inflammation are processes involved in different ocular surface diseases. Dry Eye Disease (DED) is such a disease with presence of ROS in tears and ocular surface structures, leading to activation of inflammatory signalling pathways, recruitment and infiltration of immune cells in the lacrimal glands and altered tear film (Uchino et al., 2012; Yamaguchi, 2018). This causes visual discomfort and disturbance to the patient often compromising the daily life (Seen and Tong, 2018). Mild DED cases are treated with artificial tears that modulate retention of water on the ocular surface (Kojima et al., 2020). The treatment of more serious cases is based on the use of anti-inflammatory agents, such as topical corticosteroids, cyclosporine A and lifitegrast, a small integrin antagonist. However, the active compounds or the excipients of these drugs may cause side effects and/or lack of tolerability, for instance foreign body sensation and irritation (Jones et al., 2017; Lollett and Galor, 2018), increased intraocular pressure and cataract (Lollett and Galor, 2018). Hence, there is still a demand for novel therapeutic

* Corresponding author at: IOBA, Campus Miguel Delibes, Paseo de Belen 17, 47011 Valladolid, Spain.
E-mail address: mjgonzalez@ioba.med.uva.es (M.J. González-García).

https://doi.org/10.1016/j.ijpharm.2022.122028
Received 31 March 2022; Received in revised form 13 July 2022; Accepted 14 July 2022
Available online 16 July 2022

approaches.

Polyphenols, a class of more than 10,000 secondary plant metabolites, have broad spectrum of pharmacological activities (Li et al., 2014). Polyphenols are organized in distinct groups and subgroups according to their structural complexity (Es-Safi et al., 2007). Quercetin (QUE) (2-(3,4- dihydroxyphenyl)-3,5,7-trihydroxychromen-4-one) and resveratrol (RSV) (3,5,4′ -trihydroxy-*trans*-stilbene) are polyphenolic compounds in the classes of flavonoids and stilbenes, respectively. They have anti-inflammatory, anti-oxidative, and anti-angiogenic properties that are of interest in the treatment of cancer, cardiovascular disorders, hypertension and other pathologies. (Koushki et al., 2018) Also, several studies have shown that quercetin and resveratrol have potential therapeutic application in ophthalmological diseases (Abu-Amero et al., 2016; Zhao et al., 2021). For example, resveratrol promotes an increase in the reduced glutathione (GSH) concentration in cataract model (Doganay et al., 2006). Kubota *et al.* showed that oral delivery of resveratrol was able to reduce the levels of Inter Cellular Adhesion Molecule-1 (ICAM-1) and Monocyte Chemoattractant Protein 1 (MCP-1), proteins involved in the inflammatory cascade, in a uveitis mouse model (Kubota et al., 2009). Our group showed that QUE and RSV (delivered as dilute ethanol solutions) efficiently decreased the intracellular production of ROS in HCE and IOBA-NHC cells. Furthermore, the levels of inflammatory cytokines (e.g. IL-1α) were decreased in the tear fluid of mice with experimental DED and an improvement of the corneal surface integrity was also detected (Abengózar-Vela et al., 2019). Even though our findings revealed the potential applicability of QUE and RSV as a treatment for DED, their poor physicochemical characteristics, such as low water solubility and a low chemical stability, limit their use in therapeutics. This encouraged us to investigate possible formulation strategies.

One potential strategy involves the use of cyclodextrins (CDs) (Loftsson and Stefánsson, 1997). The CDs possess a ring-shaped structure, capable of hosting lipophilic drugs in the inner cavity (Abdelkader et al., 2018; Saokham et al., 2018). This non-covalent host–guest interaction results in a dynamic equilibrium between the free and CD-complexed drug (Messner et al., 2010). CDs are widely used in pharmaceutical products for buccal, nasal or ophthalmic delivery (Del Valle, 2004). Several commercial eyedrops include CDs; for example, chloramphenicol complexed with MβCD (Chlorocil ®, Laboratório Edol) and indomethacin with HPβCD (Indocollyre®, Bausch & Lomb).

In addition to the inclusion complexes, assemblies of CDs and drug molecules can give rise to supramolecular structures in the nanoscale (Loftsson and Duchêne, 2007). Combining hydrophilic polymers to the drug:CD solutions may result in synergistic solubilization and stabilization of the drug, that is explained by the mutual interactions between the drug, CD and polymer in solution (Saokham et al., 2018). As previously reported by Jansook *et al.*, hyaluronic acid (HA) and other hydrophilic polymers efficiently stabilized binary complexes of celecoxib and CDs (Jansook et al., 2019). HA is an endogenous glycosaminoglycan in the joints and eyes. High molecular weight HA shows excellent biocompatibility, non-inflammatory and non-immunogenic characteristics. In addition, it is used as lubricant compound in the artificial tears in the treatment of DED (Bayer, 2020).

The objective of this study was to improve the solubility and stability of QUE and RSV using hydroxypropyl-β-cyclodextrin (HPβCD) and the combination of HPβCD with HA. The formulations were physiochemically characterized and their biocompatibility and intracellular antioxidant activity was evaluated in human corneal and conjunctival cell lines.

2. Materials and methods

2.1. Materials

Hydroxypropyl-β-cyclodextrin (HPβCD) (Av. Mw 1396 Da) (Degree of substitution: 0.67 hydroxypropyl groups per glucose unit), quercetin (QUE), resveratrol (RSV), 2′,7′-dichlorofluorescein diacetate (H_2DCFDA), trifluoroacetic acid (TFA), penicillin/streptomycin, human epithelial growth factor (hEGF), hyaluronic acid sodium salt (MW range 1.5–1.8 MDa), 5-methylphenazinium methyl sulphate (PMS) and bovine insulin were obtained from Merck Life Sciences (St. Louis, MO, USA). Cell culture medium Dulbecco's modified Eagle's medium/Nutrient Mixture F-12 (DMEM/F-12) + GlutaMax, DMEM/F12 without phenol red, Dulbecco's phosphate buffered saline (DPBS), fetal bovine serum (FBS), XTT ((2,3-Bis-(2-methoxy-4-nitro-5-sulfophenyl)–2*H*-tetrazolium-5-carboxanilide), human insulin, BCA Protein Assay kit and all the plastic material (tips, pipettes, culture flask and plates) were purchased from ThermoFisher Scientific (Rockford, IL, USA). MilliQ water was obtained from the Millipore unit. Acetonitrile of HPLC grade was obtained from PanReac (Darmstadt, Germany).

2.2. Physicochemical characterization of the formulations

2.2.1. Quantitative analysis of QUE and RSV

For quantitation of QUE and RSV a chromatographic method was developed based on reversed-phase high-pressure liquid chromatography (RP-HPLC) Waters e2695 separation module equipped with an autosampler and a quaternary pump, connected to a Waters 2998 photodiode array detector provided with an UV detector. A C18 Mediterranean Sea column (250 × 4.6 mm, 5 μm) (Teknokroma Analítica S. A., Barcelona, Spain) with an OptiGuard 1 mm guard column (Sigma-Aldrich, San Luis, Missouri, USA) was used for the separation. The flow rate was set to 1 mL/min and the injection volume was 20 μL. The mobile phase consisted of milliQ water/ 0.05 % (v/v) TFA (A) and acetonitrile/0.05 % (v/v) TFA (B) which were eluted in a gradient mode as follows: 4 min 10 % B, 6 min 30 % B, 16 min 60 % B, 17 min 95 % B, 18 min 95 % B, 19 min 10 % B, 22 min 10 % B. The retention time for QUE was 15.6 min, while for RSV was 14.7 min, and the wavelengths used for detection were 370 nm and 306 nm, respectively. For the acquisition and processing of data Empower® 3 software (Waters®, Ireland, UK) was used. Standard solutions of QUE (range: 1.5–30 μg/mL, linearity R^2: 0.9968; LOD −1.87 μg/mL; LOQ-2.13 μg/mL) and RSV (range: 1–35 μg/mL, linearity R^2:0.9984; LOD-3.12 μg/mL; LOQ- 4.82 μg/mL) were prepared in ACN:H_2O 50:50 (v/v) and analysed with the same conditions as the samples.

2.2.2. Chemical stability

The chemical stability of QUE and RSV in PBS (pH 7.4) in the presence of 5 % w/v of HPβCD was assessed under controlled temperature (25 °C). Additionally, the possible stabilizing effect of 0.1 %, 0.25 % and 0.5 % w/v of HA was evaluated. Solutions of free QUE and RSV were used as controls. Samples were protected from light. The clarity of all formulations was visually inspected prior to each analysis. At scheduled time points aliquots of the samples were withdrawn and quantified by RP-HPLC. Data are expressed as percentage of the initial compound concentration (C_0) at the initial time (t_0), and was properly fitted to first order degradation kinetics using the equation below:

$$\ln(C_t/C_0) = -kt \quad (1)$$

The half-life of compound degradation (t ½) represents the period in which the initial concentration of the samples is reduced by half, and was calculated as follows:

$$t_{1/2} = \ln(2)/k \quad (2)$$

Shelf-life of a compound (t_{90}) is the time in which its initial concentration decreases to 90 % of the initial one, it is calculated as shown:

$$t_{90} = 0.105/k \quad (3)$$

2.2.3. Solubility studies

The solubility of QUE and RSV in the presence of HPβCD was studied in PBS (pH 7.4). Briefly, an excess amount of QUE or RSV was added to

Table 1
Composition of binary and ternary complexes; ingredient amounts are expressed as % w/v.

Ingredient	Formulations			
	F1	F2	F3	F4
Quercetin	0.065	0.065	–	–
Resveratrol	–	–	0.35	0.35
HPβCD	5	5	5	5
HA	–	0.1	–	0.1

increasing concentrations of HPβCD up to 12.5 % (w/v). The saturated drug suspensions were left in agitation overnight at 25 °C protected from light. After this time the suspensions were centrifuged (6000 rpm, 10 min) to remove any undissolved drug and analysed for QUE and RSV concentration by RP-HPLC.

Phase solubility profiles were established following the method proposed by Higuchi and Connors (Higuchi and Connors, 1965). The apparent stability constant ($K_{1:1}$) and complexation efficiencies (CE) were calculated using equations (4) and (5), starting from the slopes of the phase solubility diagrams, where S_0 represents the solubility of the drug (Messner et al., 2010). In a specific complexation media, CE can be used for calculating the molar ratio between drug-cyclodextrin as reported in equation (6).

$$K1:1 = \frac{slope}{S_0(1 - slope)} \tag{4}$$

$$CE = \frac{\left[\frac{D}{CD}\right]}{[CD]} = S_0{}^{*}K1:1 = \frac{slope}{1 - slope} \tag{5}$$

$$D:CDmolarratio = 1:\frac{(CE+1)}{CE} \tag{6}$$

Additionally, the same studies were repeated in the presence of 0.1 % w/v HA to evaluate the effect of this polymer on QUE and RSV solubilization by HPβCD complexation.

2.2.4. Preparation of the formulations

Complexes were prepared by dissolving QUE or RSV in a solution of HPβCD in PBS under agitation. After equilibration at room temperature (RT), any undissolved drug was eliminated through centrifugation (6000 rpm, 10 min). Solid state characterization was performed on freeze-dried solutions (24 h, −50 °C) (Lyoquest-55, Telstar, Terrassa, Spain). The quantities used were chosen based on previously conducted phase solubility and stability studies. The composition of all inclusion complexes prepared is listed in Table 1.

2.2.5. Fourier Transform infrared (FT-IR) spectra analysis

The Fourier-Transform Infra-Red spectra of pure QUE, RSV, CD and HA and their lyophilized complexes were acquired with a FT-IR Bruker ALPHA spectrometer (Ettlingen, Germany). All analyses were performed at RT. Data were collected in the range of 400–4000 cm^{-1} with a spectral resolution of 4 cm^{-1} with an average of 60 scans. Data were collected and processed by OPUS software (version 7.2, Bruker Optik GmbH, Ettlingen, Germany).

2.2.6. Dynamic light scattering (DLS) measurements

Dynamic light scattering (DLS) was used for the characterization of the particle size within the formulations. All measurements were performed using a Zetasizer Pro (Malvern Panalytical, Malvern, Worcestershire, United Kingdom) in triplicate at RT with a scattering angle at 173°. Possible larger aggregates were eliminated through filtration using a 0.45 μm filter before each measurement.

2.2.7. Atomic force microscopy (AFM)

Surface topography and the size of the complexes were analysed by atomic force microscopy (AFM) (Asylum Research MFP3D BIO; Oxford Instruments, Abingdon, Oxfordshire, United Kingdom). The measurements were performed in tapping mode with 240AC-NA OPUS tips (MikroMasch). Samples were prepared by placing 20 μL of the sample on a recently cleaved mica surface and letting it evaporate at room temperature. Quantitative data, like particle size were obtained through the Gwyddion software (version 2.55, Department of Nanometrology, Czech Metrology Institute, Brno, Czech Republic).

2.3. Biological assays

2.3.1. Cell lines and culture conditions

Human corneal epithelial (HCE) (Araki-Sasaki et al., 1995) and immortalized human conjunctival epithelial (IM-ConjEpi) (Innoprot, Derio, Spain) cell lines were used to evaluate the biocompatibility and functional performance of formulations. Both cell lines are SV-40 Large T antigen immortalized cell lines.

HCE cells were cultured in DMEM/F-12 + GlutaMax cell medium supplemented with 10 % FBS, 5 μg/mL human insulin, 10 ng/mL EGF and with 100 U/mL of penicillin and 0.1 mg/mL of streptomycin. The passages used were from 35 to 45.

IM-ConjEpi cells were cultured in DMEM/ F-12 + GlutaMax which was completed with 10 % FBS, 10 ng/mL EGF, 1 μg/mL bovine insulin and 5000 U/mL of penicillin and 5000 μg/mL of streptomycin. The passages used were from 7 to 15.

The two cell lines were cultured at controlled temperature and atmosphere (37 °C, 5 % CO_2). Quotidian inspection of the cells was performed under the phase contrast microscope, while the cell medium was exchanged on every second day.

2.3.2. Cell viability

To determine the cell viability of HCE and IM-ConjEpi cells after exposure to the different formulations a XTT cell viability assay was performed. Cells were seeded in 96-well plates ($1x10^4$ cells/well) and grown in supplemented medium until 90 % of confluence was reached. Cells were then maintained in supplement-free medium for 24 h. Afterwards, cells were exposed to the formulations (Table 1) for 24 h. In all cases final concentrations of the polyphenols in the complexes were adjusted in accordance with our previous study (Abengózar-Vela et al., 2015). Concentration range of QUE was 0–50 μM and 0–300 μM for RSV in the complexes. As negative and positive controls, cells were exposed to cell culture medium or 0.005 % benzalkonium chloride (BAK), respectively. After 24 h exposure, cell viability was measured as follows. In brief, cell culture supernatants were discarded, and the wells were loaded with 100 μL of DMEM/F-12 without phenol red. Then, 25 μL of PMS/XTT reaction mixture (10 μL of 3 mg/mL of PMS in 0.25 mg/mL of XTT) prepared just before use was added to each well. After the addition of the reaction mixture the cells were incubated at 37 °C for 3 h. UV/Vis spectrophotometer (SpectraMax M5; Molecular Devices, Sunnyvale, CA, USA) was used for the measurement of the absorbance at 450 and 660 nm, respectively. The percentage of living cells was calculated relative to the values of the negative control. Six replicates were performed in three independent experiments for each formulation.

2.3.3. Intracellular ROS scavenging activity

Intracellular ROS scavenging capacity of the formulations was measured using H_2DCF-DA. HCE and IM-ConjEpi cells were cultured into 24-well plates ($6x10^4$ cells/well) until 90 % of confluence was reached. After this, the cells were maintained in non-supplemented medium for 24 h. Subsequently, the cells were pre-treated with 500 μL of the formulations and left for 1 h at 37 °C. The formulations were then removed, and the cells were incubated for 30 min with 500 μL of a 10 μM solution of H_2DCF-DA. After 30 min the H_2DCF-DA solution was removed, and the cells were treated again with the formulations (at the same concentration as before) and exposed to 8-W UV-B lamp (Bio-Rad, Inc., Hercules, CA, USA) for 15 s. Control cells were not irradiated. After the UV-B exposure the cells were cultured for 1 h. The intracellular

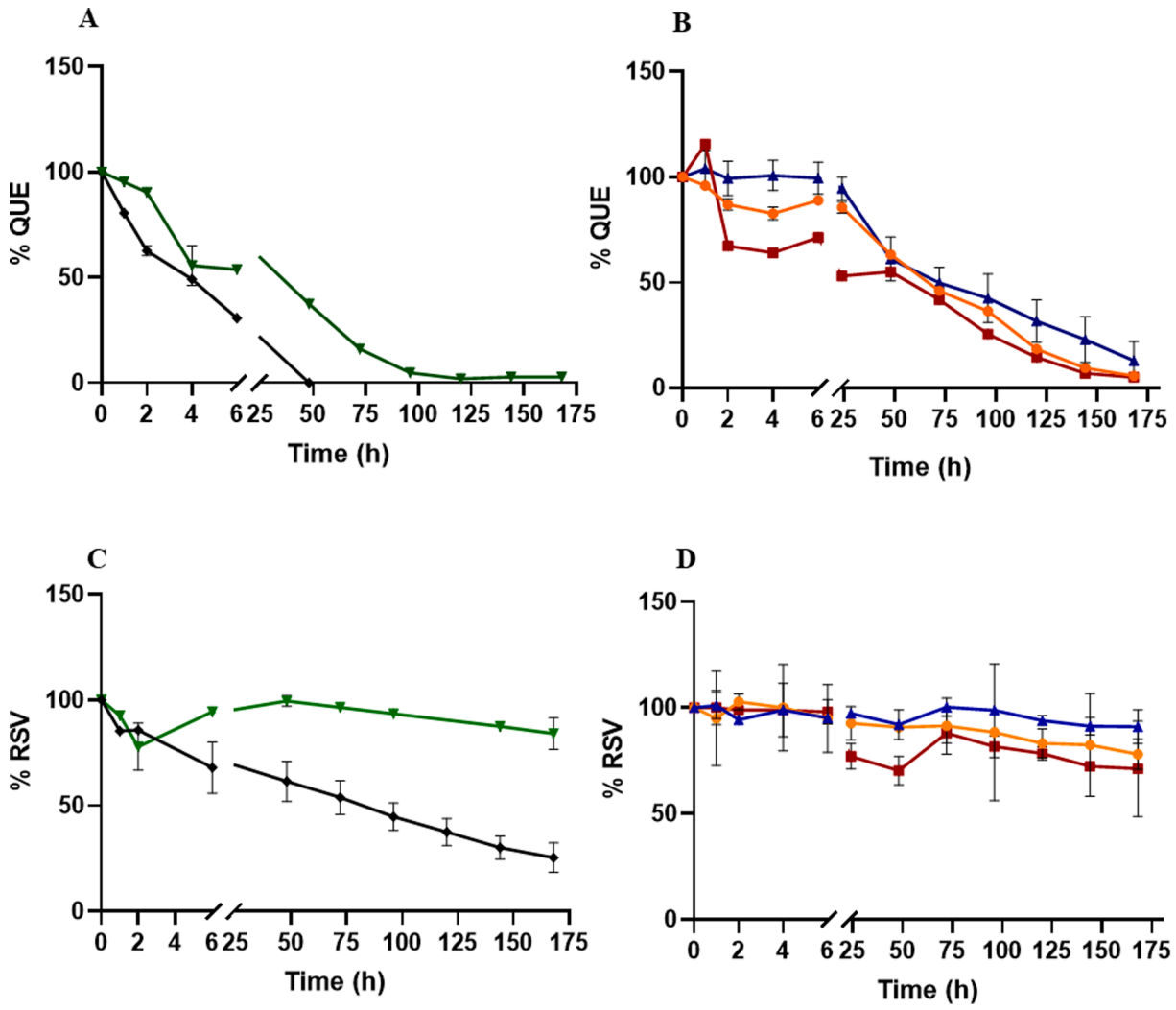

Fig. 1. Stability profiles (25 °C, pH 7.4) of **A**- pure QUE (◆), with HPβCD (▼) **B**- QUE with HPβCD:HA: 0.1 % of HA(▲), 0.25 % of HA (●) and 0.5 % of HA w/v (■). Stability profiles of **C**- pure RSV (◆), with HPβCD (●) **D**- RSV with HPβCD:HA: 0.1 % of HA(▲), 0.25 % of HA (●) and 0.5 % of HA w/v (■). Each point represents the % of QUE or RSV at a given time point in respect to the initial concentration and these are means of three measurements ± SEM.

fluorescence intensity was measured at 488 nm (excitation) and 522 nm (emission). The data obtained from the fluorescence measurements were normalized by the total protein content. The latter was measured in adherent cells using the BCA assay, following the manufacturer's instructions. For each treatment two replicates were performed in three independent experiments for each formulation.

2.4. Statistical analysis

All experiments were performed in triplicate (n = 3) and data are represented as mean ± standard error of the mean (SEM). The SPSS software was used (SPSS 20.0; SPPS, Inc., Chicago, IL, USA) for the statistical analysis applying one-way analysis of variances (ANOVA) followed by Tukey's or Games-Howell post-hoc tests.

3. Results and discussion

3.1. Chemical stability of complexed QUE and RSV

To study the short-term chemical stability of complexed and pure QUE and RSV, all samples were placed in glass vials, protected from

Table 2
Summary of the first order degradation constant (k), half-time degradation period ($t_{½}$), shelf-life (t_{90}) and the correlation coefficient (R^2) for pure QUE and RSV and complexes with HPβCD and HPβCD:HA in PBS (pH 7.4) at 25 °C. All concentrations are expressed as % w/v and all samples contained 5 % w/v HPβCD.

Sample	Additive HA	k (h^{-1})	$t_{1/2}$ (h)	t_{90} (h)	R^2
Pure QUE	–	0.188	3.66	0.55	0.987
QUE: HPβCD	–	0.029	23.57	3.57	0.940
QUE: HPβCD:HA	0.1 %	0.012	55.45	8.75	0.967
	0.25 %	0.015	44.71	6.77	0.946
	0.5 %	0.016	43.05	6.52	0.941
Pure RSV	–	0.0071	97.62	14.78	0.967
RSV: HPβCD	–	0.0009	770.16	116.66	0.819
RSV: HPβCD:HA	0.1 %	0.0008	866.43	131.25	0.900
	0.25 %	0.0013	533.19	80.76	0.908
	0.5 %	0.0018	385.08	58.33	0.613

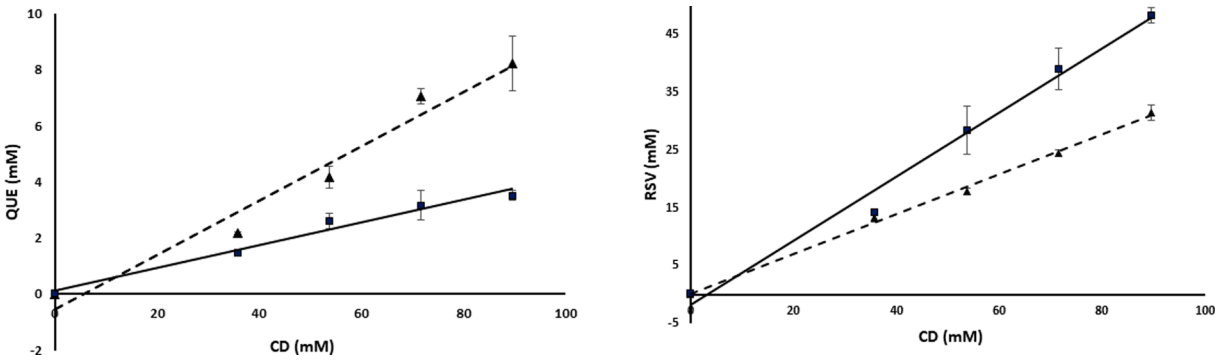

Fig. 2. Phase solubility studies (25 °C, pH 7.4) of QUE with A: HPβCD (■) and HPβCD:HA (▲). B: RSV with HPβCD (■) and HPβCD:HA (▲).

light, and kept in a controlled environment room. Additionally, the possible stabilizing effects of different concentrations of HA were evaluated. One-week stability profiles are reported in Fig. 1. Table 2 summarizes the kinetic parameters of the degradation reactions.

Pure QUE was unstable in aqueous solution at 25 °C. The calculated kinetic parameters showed that the half-life ($t_{½}$) is 3.66 h, meaning that basically all QUE degrades in less than one day. The degradation was slower when QUE was complexed with HPβCD and HPβCD:HA. The degradation half-life of QUE was prolonged to about one day for the complexes with HPβCD. The stabilizing effect of HA was inversely proportional to its concentration as the best stabilization of QUE was seen at the lowest HA concentration (0.1 % w/v). Chromatograms of pure QUE showed the onset of lower retention peaks than the one of QUE after 24 h, meaning that the degradation products formed are more hydrophilic than pure QUE. Although these products were not determined in detail (beyond the scope of this study) this finding corroborates the theory that the main pathways of degradation of QUE are oxidation and hydroxylation.

In the case of RSV, the pure compound showed to be more stable than pure QUE, having a degradation half-life of 97.6 h. Complexes of RSV with HPβCD and HPβCD:HA showed to enhance the stability of the polyphenol and this improvement was dependent on the HA concentration.

Various authors reported that the stability of QUE is influenced by the temperature and pH of solution. For example, Wang *et al.* showed that QUE followed a first-order kinetics of degradation upon incubation at 37 °C. The same authors reported that the degradation rate decreased at lower pH (6 and 6.8). Some authors proposed the addition of proteins, like casein (Wang and Zhao, 2016; Wang et al., 2016) as a potential strategy to stabilize QUE. In addition to the exposure to UV or visible light, which triggers the conversion from *trans*- to *cis*-RSV, other environmental factors, like pH and temperature, influence the RSV stability. The phenolic groups of RSV ionize at basic pH leading to the formation of the phenate ions more prone to oxidation compared to the protonated form of RSV. Therefore, at more acidic pH (<6.8) RSV seems to be stable since all the phenolic groups are in their non-ionized form (Robinson, 2015; Zupančič et al., 2015). The higher instability of QUE compared to that of RSV can be explained by the comparison of their chemical structure: QUE possesses more hydroxyl groups (5 groups) than RSV (3 groups). A greater number of hydroxyl groups leads to an easier oxidation (Sokolová et al., 2011). This explains well the stability profiles of the pure compounds observed in our studies. All subsequent studies were performed with 0.1 % w/v HA as it displayed the higher stabilizing capacity in the case of both polyphenolic compounds. It is interesting to notice that a higher stabilization of the two polyphenols was achieved at the lowest concentration of HA (0.1 % w/v) in solution. This can be justified by the fact that a higher concentrations HA is able to form intra- or intermolecular hydrogen bonds leading to the formation of a three-dimensional polymeric web. In this case less HA is accessible to interact and stabilize the polyphenolic compounds (Snetkov et al., 2020).

Formation of binary or tertiary complexes of QUE or RSV with CD or CD: hydrophilic polymers, respectively, has emerged as an interesting approach to enhance the stability profiles of these compounds and we are not aware of the previous drug stability reports in this respect.

3.2. Solubility of QUE and RSV in the formulations

The effect of increasing concentrations of HPβCD (0–12.5 % w/v) on the solubility of QUE and RSV in PBS (pH 7.4) was investigated in phase-solubility experiments (Fig. 2). Among different CDs, we selected HPβCD due to its safety in eyedrop formulations and by ability to increase absorption of hydrophobic drugs to the eye (Challa et al., 2005).

The phase solubility profiles of QUE indicate linear solubility improvement with increasing concentration of HPβCD. Thus, the profile is in accordance with the A_L type complexation in the classification of Higuchi and Connors. Stability constant $K_{1:1}$ of the association between QUE and HPβCD was 2609 M^{-1}. However, in the case of poorly soluble drugs like QUE, the determination of intrinsic solubility (S_0) is not always accurate. Since this value is used for the calculation $K_{1:1}$ this can lead to an over- or underestimation of the complexation capacity. Calculation of CE represents a more exact parameter of the estimation of the solubilizing efficiency of the CDs (Loftsson and Brewster, 2012). This value (eqn. (4)) is independent of S_0. In this case, CE was calculated to be

Table 3
Results from the phase-solubility studies measured at 25 °C and pH 7.4 (mean ± SEM; n = 3).

Polyphenol	HA (% w/v)	Type	$K_{1:1}$ (M^{-1})	CE	Drug:CD molar ratio	Solubility (mg/mL) in the presence of 5 % (w/v) CD	Solubility (mg/mL) in the presence of 12.5 % (w/v) CD
QUE[a]	–	A_L	2609	0.04	1:24	0.44 ± 0.09	1.06 ± 0.28
QUE[a]	0.1	A_L	7940	0.10	1:10	0.65 ± 0.03	2.48 ± 0.99
RSV[a]	–	A_L	9808	1.24	1:1.8	3.24 ± 0.41	11 ± 3.6
RSV[a]	0.1	A_L	7299	0.52	1:2.9	3.04 ± 0.78	7.17 ± 1.25

[a] all complexes were prepared with HPβCD (0–12.5 % w/v).

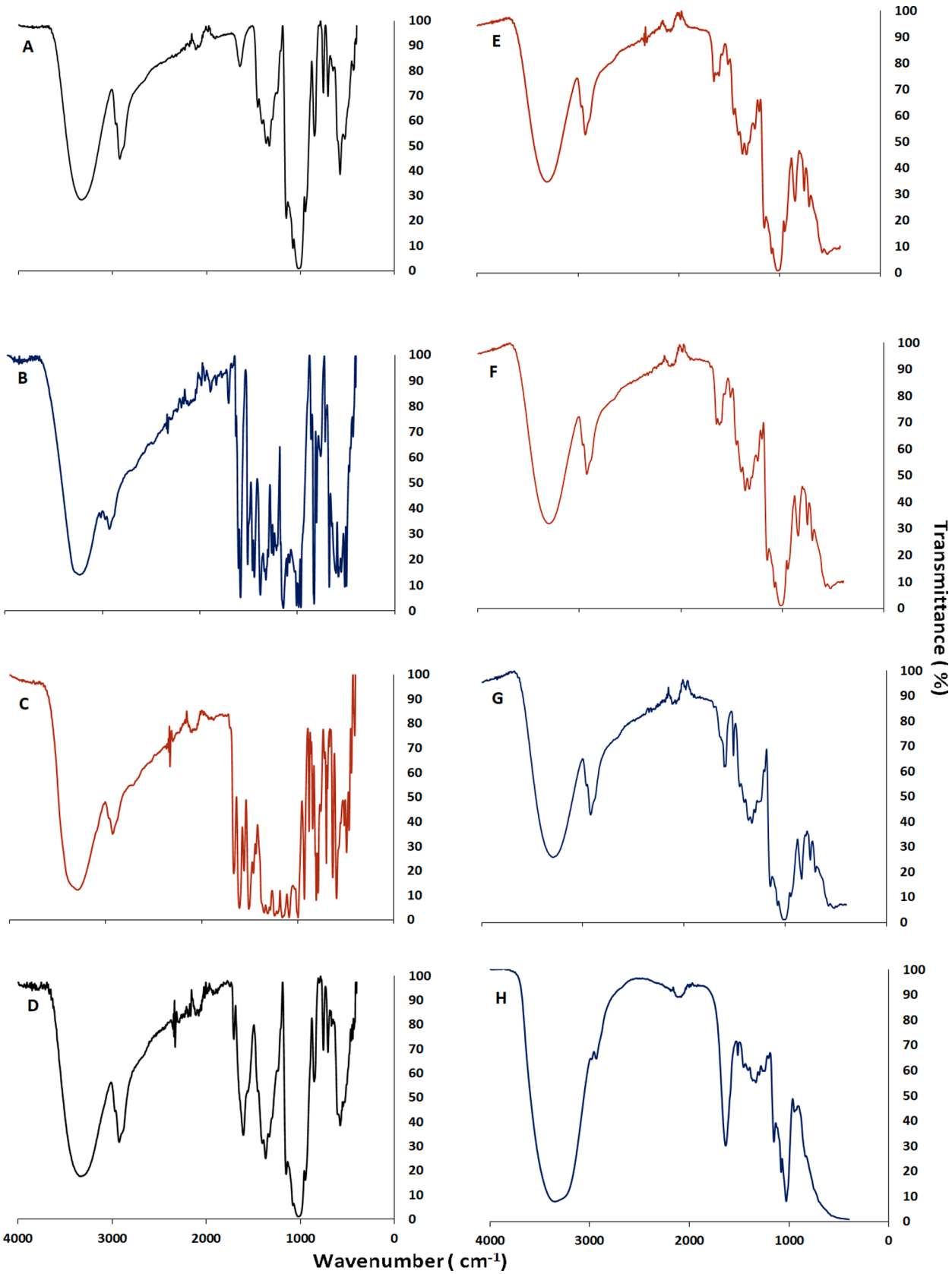

Fig. 3. FT-IR spectra of pure HPβCD (A), RSV (B), QUE (C), HA (D) and complexes of RSV with HPβCD (E) and HPβCD:HA (F) and QUE with HPβCD (G) and HPβCD: HA (H).

Table 4
Hydrodynamic diameter (d),the intensity distribution (%I) and d10, d50 and d90 values for all the formulations measured by DLS (mean ± SEM; n = 3).

Formulation	d (nm)	%I	d10	d50	d90
QUE: HPβCD complexes	2.81 ± 0.23	93.1	1.645 ± 0.099	2.735 ± 0.18	303.29 ± 298.0.51
	3647 ± 418.8	6.86			
QUE: HPβCD:HA complexes	2.08 ± 0.006	63	1.47 ± 0.026	2.58 ± 0.02	135.76 ± 0.89
	103.6 ± 1.31	34.78			
RSV: HPβCD complexes	2.74 ± 0.1	98.65	1.50 ± 0.082	2.54 ± 0.088	4.49 ± 0.30
	3804 ± 211.5	2.024			
RSV: HPβCD:HA complexes	2.22 ± 0.005	61.38	1.62 ± 0.072	2.80 ± 0.03	109.53 ± 3.24
	82.14 ± 1.32	36.13			

0.04 and the drug:CD molar ratio 1:25. If the formation of 1:1 drug:CD soluble complex is assumed, one out of every 25 cyclodextrin molecules is involved in the complex formation (Loftsson et al., 2005). In the case of RSV, the values of $K_{1:1,}$ CE, and drug:CD ratio were 9808 M^{-1}, 1.24 and 1.8. This suggests that the complexation of RSV with CD is more efficient than in the case of QUE.

The introduction of excipients, such as hydrophilic polymers has been indicated to improve the solubilization capacity of CDs. In addition, this promotes formation of complexed particle-like structures. The addition of hyaluronic acid (HA) resulted in further improvement in the solubility of QUE. For example, at the highest concentration of HPβCD (12.5 % w/v) the solubilized quantity of QUE increased from 0.44 mg/mL to 1.06 mg/mL. This was reflected in the values of $K_{1:1}$ and CE, which were 7940 M^{-1} and 0.1, respectively. Greater CE values indicate that smaller number of CD molecules are required in QUE solubilization, and that the complexation is more effective. On the contrary, the presence of HA slightly reduced the solubilization and complexation of RSV. In this case $K_{1:1}$ and CE were 7299 M^{-1} and 0.52, i.e. values moderately lower than without HA. Table 3 summarizes all the parameters calculated from the phase solubility diagrams.

3.3. Fourier transformed infrared spectroscopy

Fourier transformed infra-red (FT-IR) spectroscopy was used to confirm the presence of both host and guest molecules in the inclusion complexes. Fig. 3 illustrates the spectra of free QUE, RSV, HPβCD and HA, together with the spectra of the complexes. The spectrum of pure QUE shows the characteristic bands: stretching of the hydroxyl groups was detected in the region between 3400 and 3200 cm^{-1}. The intense bending of the phenolic hydroxyl was observed at around 1380 cm^{-1}. The bands corresponding to the in- and out- of plane bending of the aromatic C—H were identified in the region from 950 to 600 cm^{-1}. The signal from the ketone was detectable at 1660 cm^{-1}. With regard to the signals of pure RSV the stretching of the aromatic double C—C bonds was visible at 1600 cm^{-1}, whereas a strong signal at 960 cm^{-1} indicates stretching of the olefinic C—H. At 3200 cm^{-1} a strong broad peak of –OH group is visible.

The spectra of the pure compounds were compared with the complexed form in which we can observe different changes. It is evident the masking of the signals of the fingerprint region (1500–900 cm^{-1}) of both compounds upon complexation. The spectra of both complexes (QUE: HPβCD and RSV: HPβCD) are similar with the one of free HPβCD, with the broad and intense band of the hydroxyl groups at 3400–3200 cm^{-1} and the stretching of the –CH and $–CH_2$ groups at 2800 cm^{-1}. FT-IR spectrum of pure HA shows the bands of –OH and –NH stretching at 3400 cm-1, while the medium band intensity at 2900 cm-1 indicates the stretching of the –CH and $–CH_2$, as in the spectrum of the pure HPβCD. The wide band in the region of 1600–1500 cm-1 is representative of the amide functional group present in the backbone of *N*-acetylglucosamine. In the complexes where HA was present these bands were conserved. The spectra of QUE and RSV when complexed with either HPβCD or HPβCD:HA represent major changes in the fingerprint region, indicating that the complexation has occurred.

3.4. Particle size characterization

The size distributions of the formulations are shown in the Table 4. Binary complexes between the polyphenols and HPβCD displayed a uniform size distribution, all in the range of 2–3 nm. On the contrary, complexes containing HA exhibited bimodal particle size distribution, with an intensity peak at around 2 nm, which as in the binary complexes probably represents the monomeric complex between the drug: HPβCD,

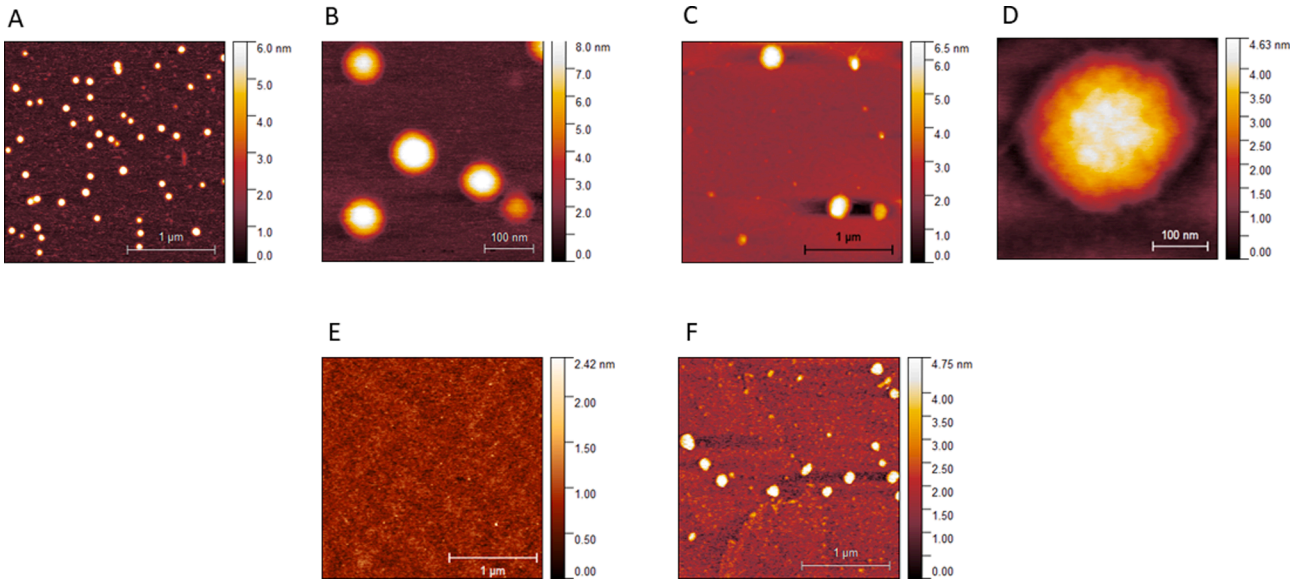

Fig. 4. AFM images of QUE in complex with HPβCD (A and B) and with HPβCD:HA (C and D); RSV in complex with HPβCD (E) and with HPβCD:HA (F). Horizontal (length) and vertical (height) scales are reported on the images.

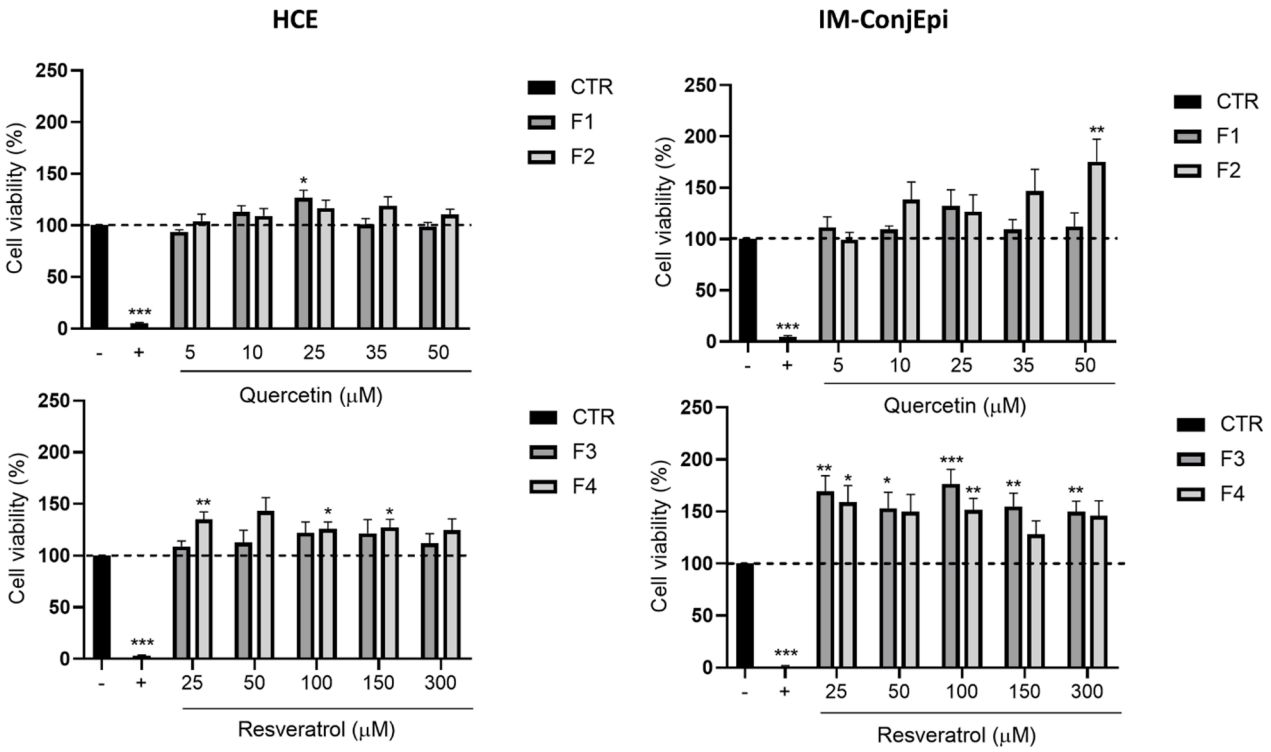

Fig. 5. Viability of HCE and IM-ConjEpi cells after treating with the formulations: F1-QUE: HPβCD, F2-QUE: HPβCD:HA, F3-RSV:HPβCD and F4-RSV:HPβCD:HA complexes, negative CTR-cell culture medium, positive CTR- BAK (0.005 %). The data represent the mean of three independent experiments ± SEM. * $p < 0.05$, ** $p < 0.01$, *** $p < 0.001$ compared with control cells treated with culture medium.

while the second intensity peak that appears represents larger complex aggregates. In addition, QUE-containing complexes were able to form slightly larger aggregates that those formed in RSV-containing complexes, 103 and 82 nm respectively. These results suggest that HA triggers formation of nanoaggregates in drug:CD complexes. The size of these aggregates are clearly below the acceptable size limit (diameter of 10 μm) in topical suspension delivery (Kassem et al., 2007).

3.5. Atomic force microscopy (AFM)

The images of the surface morphology of drug: HPβCD complexes and their aggregates were acquired with AFM. Que:HPβCD formed spherical particle-like aggregates (Fig. 4A and 4B), while the addition of HA in the complex, induced the formation of larger aggregates (Fig. 4C and 4D) of around 200 nm in diameter. Regarding the formulations containing RSV, no aggregate formation (Fig. 4E) occurred in the inclusion complexes with CD, while the ones including HA had a regular spherical shape and a diameter in the range of 40–70 nm (Fig. 4F). Size data obtained by AFM imaging confirmed the size distribution of the complexes and their aggregates previously obtained by the dynamic light scattering.

The formation of nanoaggregate structures may indicate that the improvement of solubility and stability of the two polyphenols occurs through the formation of non-inclusion complexes or micellar-like structures (Jansook et al., 2019). This could be positively reflected on the potential topical administration of the formulations since a higher corneal retention and thus an increased ocular bioavailability of QUE and RSV might be observed (Jóhannsdóttir et al., 2015).

3.6. In vitro biocompatibility of inclusion complexes

The in vitro biocompatibility of the inclusion complexes of QUE and RSV on two human ocular surface cell lines, HCE (corneal) and IM-ConjEpi (conjunctival) after a 24-hour exposure was assessed using the XTT cell viability assay. Cell viability after exposure to all complexes are shown in Fig. 5. None of the formulations reduced the cell viability of the two cell lines, that was maintained around 100 %. As expected, BAK, which was used as a positive control of toxicity, significantly decreased the viability of both cell lines ($p < 0.001$).

RSV-containing inclusion complexes seem to stimulate cell proliferation. Similar behaviour of HCEs cells was noticed by Li et al. (2020) when investigating the cytotoxicity of a micellar-based formulation of RSV (Li et al., 2020). On the other hand, the IM-ConjEpi cells seem to be more susceptible to stimulation of cell proliferation than HCE cells. It is interesting to observe that the formulations with HA promoted cell proliferation more than those without HA. This might be explained by the presence of HA specific CD44 receptor, present on the surface of human corneal and conjunctival epithelial cells (Contreras-Ruiz et al., 2011). Besides being implied in physiological processes like haematopoiesis and lymphocyte activation, HA also stimulates cell proliferation and adhesion (Jordan et al., 2015). Even though the possible generation of degradation products that can arise in QUE containing complexes, they did not affect the cellular viability of HCE and IM-ConjEpi cells in our experiments.

3.7. Intracellular antioxidant activity of formulations

H_2DCF-DA, a fluorogenic dye sensitive to ROS, was used to assess the potential intracellular free radical scavenging ability of the complexes (Table 1). H_2DCF-DA can passively diffuse into the cells, where the acetyl groups are cleaved through the action of intracellular esterase yielding a non-fluorescent compound (DCFH). DCFH is subsequently oxidized to DCF, emitting a fluorescent signal proportional to ROS levels in the cytosol (Kim, Hyeoncheol Xue, 2021). Fig. 6 illustrates the production of ROS in HCE and IM-ConjEpi cells after treatment with the formulations. The results are expressed as percentages, taking as 100 % of ROS production cells exposed to culture medium.

Binary complexes of QUE and RSV were capable to scavenge

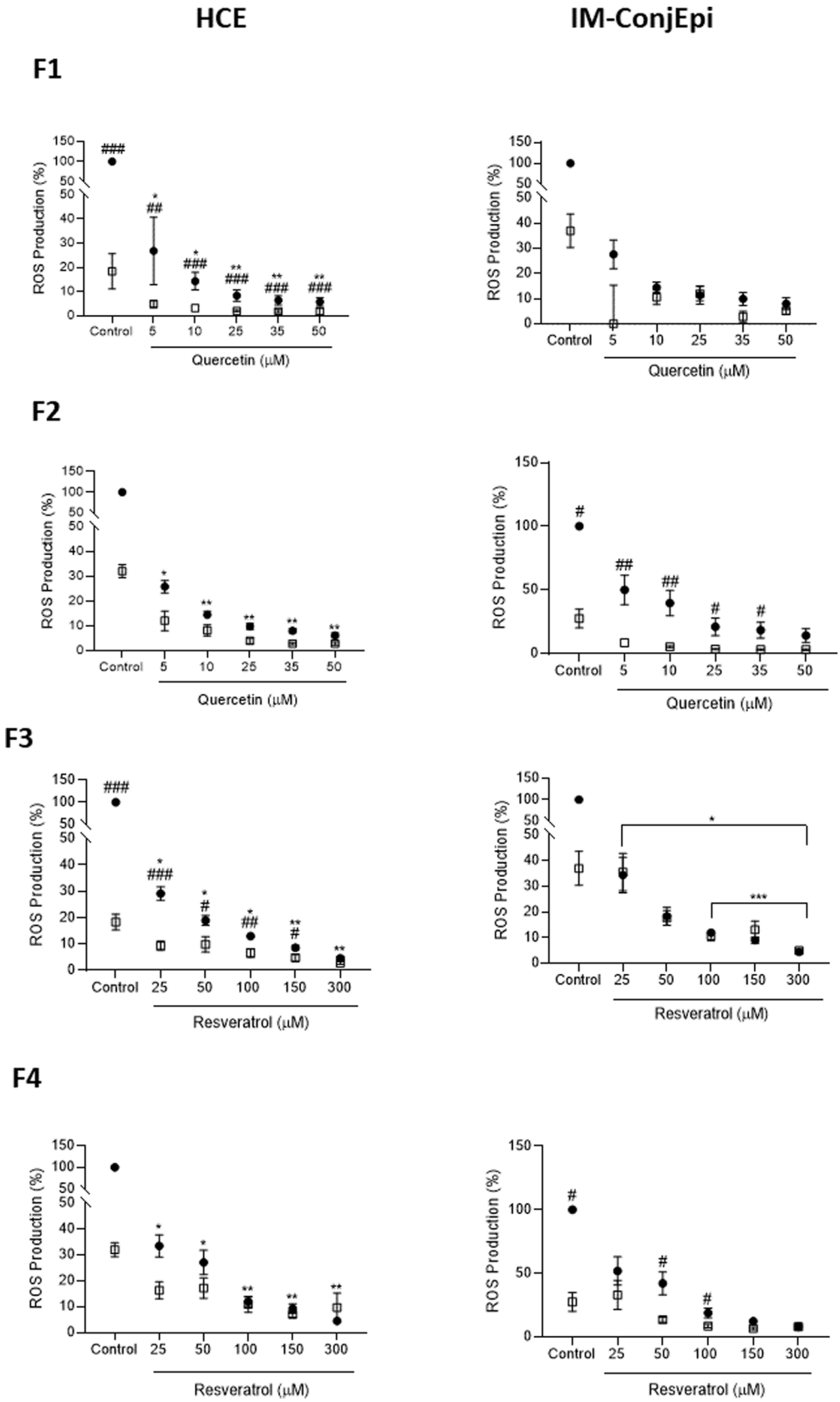

Fig. 6. Antioxidant ability of the formulations in HCE and IM-ConjEpi cells: F1-QUE: HPβCD, F2-QUE: HPβCD:HA, F3-RSV:HPβCD and F4-RSV:HPβCD:HA complexes, CTR-cell culture medium. (●) Exposed to UV-B; (▫) Unexposed to UV-B. The data represent the mean of three independent experiments ± SEM. * $p < 0.05$, ** $p < 0.01$, *** $p < 0.001$, compared with UV-B exposed cells; # $p < 0.05$, ## $p < 0.01$, ### $p < 0.001$, intergroup comparison.

cytosolic ROS in HCE cells in a dose dependent manner. A marked reduction of ROS was observed from the lowest concentrations tested ($p < 0.05$). Regarding tertiary complexes, the addition of HA did not affect the antioxidant ability of the complexes, maintaining it to levels comparable to the ones in binary complexes. In contrast, inclusion complex with QUE reached a plateau in their antioxidant scavenging capacity when the IM-ConjEpi cells were treated with a concentration of 10 μM or higher. Inclusion complexes containing RSV, were able to reduce intracellular ROS levels with a considerably effect. In fact, statistically significant differences were observed when comparing the antioxidant effect between the highest (300 μM) and the lowest concentrations (25 μM) tested ($p < 0.005$) of RSV:HPβCD complexes, and between 50 μM and 300 μM concentrations ($p < 0.001$), as well.

All formulations demonstrated scavenging capacity of ROS. QUE and RSV exert their antioxidant activities through specific moieties and functional groups present in their chemical structure like the catechol group and the chromen-4-one nucleus in QUE, and the phenolic groups present in RSV (Amorati et al., 2017; Salehi et al., 2018). Except the alteration of the physiological balance between antioxidant enzymes and ROS, matrix-remodelling and inflammatory factors contribute to the oxidative stress in DED (Favero et al., 2021). Consequently, natural therapeutic agents capable of counterbalance this type of stress would represent a novel potential line of treatments for DED.

Due to many beneficial health effects of QUE and RSV, their potential applicability in the treatment of ophthalmic diseases, especially those affecting the ocular surface like DED was proposed in this study. Issues related to their physico-chemical characteristics, like poor water solubility were successfully solved through the formation of binary or tertiary complexes with HPβCD and HPβCD:HA. Also, the formation of tertiary complexes with HPβCD:HA showed to be more advantageous in terms of chemical stability improvement of the two compounds. Therefore, it should be considered as a good starting point for future formulation solutions. In the case of QUE the stability improvement observed was of modest extent and additional efforts in stabilizing it are needed. For RSV, a greater stabilizing effect was achieved. The shelf-lives (t_{90}) found for ternary complexes were 8.75 h for QUE:HPβCD:HA and 131. 25 h (5.5 days) for RSV:HPβCD:HA. These results suggest that

slight modifications of some parameters like the pH or the addition of chelating agents, such as EDTA, could lead to an adequate stability period, which for eye drops formulation should be around one year (considering the allowed limit of degradation of 10 %). An alternative approach involves lyophilized powder, if the stability after reconstitution can be maintained for at least one month. It has to be underlined that due to the low chemical stability of the two compounds, especially QUE, the results in many literature studies may represent the effects of the degradation products, instead of biological effects of QUE.

4. Conclusions

The aim of this study was to develop a simple strategy to improve the topical ophthalmic delivery of two hydrophobic polyphenolic compounds, quercetin, and resveratrol. For this purpose, binary and tertiary inclusion complexes with HPβCD and HPβCD:HA were prepared. For both compounds tertiary complexes exhibited a greater stabilizing effect than the secondary ones. In vitro studies proved that the formulations are biocompatible with human corneal and conjunctival epithelial cells and that they have a notable ability to scavenge intracellular ROS. Although the properties of both compounds improved through the formation of complexes, we think that the ones containing RSV have a higher potential applicability in the treatment of DED, since they are more stable and less challenging for the formulator and further prospective scale-up.

CRediT authorship contribution statement

Luna Krstić: Conceptualization, Methodology, Investigation, Resources, Data curation, Writing – original draft, Visualization. **Pekka Jarho:** Methodology, Writing – review & editing, Supervision. **Marika Ruponen:** Methodology, Writing – review & editing, Supervision. **Arto Urtti:** Conceptualization, Writing – review & editing, Funding acquisition. **María J. González-García:** Conceptualization, Writing – review & editing, Supervision, Funding acquisition, Project administration. **Yolanda Diebold:** Conceptualization, Writing – review & editing, Supervision, Funding acquisition.

Declaration of Competing Interest

The authors declare that they have no known competing financial interests or personal relationships that could have appeared to influence the work reported in this paper.

Data availability

Data will be made available on request.

Acknowledgment

We thank Javier Gutiérrez Reguera for his help with the AFM experiments and data interpretation. We also, thank the High-Pressure Processes Group from the University of Valladolid for kindly allow us to use RP-HPLC and FT-IR equipment.

Funding

This work was funded by H2020 Marie Skłodowska-Curie Actions, grant number 765608 and by the Spanish Ministry of Science, Innovation and Universities and European Regional Development Fund, RTI2018-094071-B-C21.

References

Abdelkader, H., Fathalla, Z., Moharram, H., Ali, T.F.S., Pierscionek, B., 2018. Cyclodextrin enhances corneal tolerability and reduces ocular toxicity caused by diclofenac. Oxid. Med. Cell. Longev. 2018, 1–13.

Abengózar-Vela, A., Calonge, M., Stern, M.E., González-García, M.J., Enríquez-De-Salamanca, A., 2015. Quercetin and resveratrol decrease the inflammatory and oxidative responses in human ocular surface epithelial cells. Investig. Ophthalmol. Vis. Sci. 56, 2709–2719. https://doi.org/10.1167/iovs.15-16595.

Abengózar-Vela, A., Schaumburg, C.S., Stern, M.E., Calonge, M., Enríquez-de-Salamanca, A., González-García, M.J., 2019. Topical Quercetin and Resveratrol Protect the Ocular Surface in Experimental Dry Eye Disease. Ocul. Immunol. Inflamm. 27, 1023–1032. https://doi.org/10.1080/09273948.2018.1497664.

Abu-Amero, K.K., Kondkar, A.A., Chalam, K.V., 2016. Resveratrol and ophthalmic diseases. Nutrients 8, 1–16. https://doi.org/10.3390/nu8040200.

Amorati, R., Baschieri, A., Cowden, A., Valgimigli, L., 2017. The antioxidant activity of quercetin in water solution. Biomimetics 2, 6–9. https://doi.org/10.3390/biomimetics2030009.

Araki-Sasaki, K., Ohashi, Y., Sasabe, T., Hayashi, K., Watanabe, H., Tano, Y., Handa, H., 1995. An SV40-immortalized human corneal epithelial cell line and its characterization. Investig. Ophthalmol. Vis. Sci. 36, 614–621.

Batliwala, S., Xavier, C., Liu, Y., Wu, H., Pang, I.-H., 2017. Involvement of Nrf2 in ocular diseases. Oxid. Med. Cell. Longev. 2017, 1–18.

Bayer, I.S., 2020. Hyaluronic acid and controlled release: A review. Molecules 25 (11), 2649.

Cabrera, M.P., Chihuailaf, R.H., 2011. Antioxidants and the integrity of ocular tissues. Vet. Med. Int. 2011, 1–8.

Challa, R., Ahuja, A., Ali, J., Khar, R.K., 2005. Cyclodextrins in drug delivery: An updated review. AAPS PharmSciTech 6, 329–357. https://doi.org/10.1208/pt060243.

Contreras-Ruiz, L., de la Fuente, M., Párraga, J.E., López-García, A., Fernández, I., Seijo, B., Sánchez, A., Calonge, M., Diebold, Y., 2011. Intracellular trafficking of hyaluronic acid-chitosan oligomerbased nanoparticles in cultured human ocular surface cells. Mol. Vis. 17, 279–290.

Del Valle, E.M.M., 2004. Cyclodextrins and their uses: A review. Process Biochem. 39, 1033–1046. https://doi.org/10.1016/S0032-9592(03)00258-9.

Doganay, S., Borazan, M., Iraz, M., Cigremis, Y., 2006. The effect of resveratrol in experimental cataract model formed by sodium selenite. Curr. Eye Res. 31, 147–153. https://doi.org/10.1080/02713680500514685.

Es-Safi, N.E., Ghidouche, S., Ducrot, P.H., 2007. Flavonoids: Hemisynthesis, reactivity, characterization and free radical scavenging activity. Molecules 12, 2228–2258. https://doi.org/10.3390/12092228.

Favero, G., Moretti, E., Krajčíková, K., Tomečková, V., Rezzani, R., 2021. Evidence of polyphenols efficacy against dry eye disease. Antioxidants 10, 1–17. https://doi.org/10.3390/antiox10020190.

Jansook, P., Kulsirachote, P., Asasutjarit, R., Loftsson, T., 2019. Development of celecoxib eye drop solution and microsuspension: A comparative investigation of binary and ternary cyclodextrin complexes. Carbohydr. Polym. 225, 115209 https://doi.org/10.1016/j.carbpol.2019.115209.

Jóhannsdóttir, S., Jansook, P., Stefánsson, E., Loftsson, T., 2015. Development of a cyclodextrin-based aqueous cyclosporin A eye drop formulations. Int. J. Pharm. 493, 86–95. https://doi.org/10.1016/j.ijpharm.2015.07.040.

Jones, L., Downie, L.E., Korb, D., Benitez-del-Castillo, J.M., Dana, R., Deng, S.X., Dong, P. N., Geerling, G., Hida, R.Y., Liu, Y., Seo, K.Y., Tauber, J., Wakamatsu, T.H., Xu, J., Wolffsohn, J.S., Craig, J.P., 2017. TFOS DEWS II Management and Therapy Report. Ocul. Surf. 15, 575–628. https://doi.org/10.1016/j.jtos.2017.05.006.

Jordan, A.R., Racine, R.R., Hennig, M.J.P., Lokeshwar, V.B., 2015. The role of CD44 in disease pathophysiology and targeted treatment. Front. Immunol. 6, 1–14. https://doi.org/10.3389/fimmu.2015.00182.

Kassem, M.A., Abdel Rahman, A.A., Ghorab, M.M., Ahmed, M.B., Khalil, R.M., 2007. Nanosuspension as an ophthalmic delivery system for certain glucocorticoid drugs. Int. J. Pharm. 340, 126–133. https://doi.org/10.1016/j.ijpharm.2007.03.011.

Kim, H.X., X.,, 2021. Detection of Total Reactive Oxygen Species in Adherent Cells by 2',7'-Dichlorodihydrofluorescein Diacetate Staining. J Vis Exp.

Kojima, T., Dogru, M., Kawashima, M., Nakamura, S., Tsubota, K., 2020. Advances in the diagnosis and treatment of dry eye. Prog. Retin. Eye Res. 78, 100842.

Koushki, M., Amiri-Dashatan, N., Ahmadi, N., Abbaszadeh, H.A., Rezaei-Tavirani, M., 2018. Resveratrol: A miraculous natural compound for diseases treatment. Food Sci. Nutr. 6, 2473–2490. https://doi.org/10.1002/fsn3.855.

Kubota, S., Kurihara, T., Mochimar, H., Satofuka, S., Noda, K., Ozawa, Y., Oike, Y., Ishida, S., Tsubota, K., 2009. Prevention of ocular inflammation in endotoxin-induced uveitis with resveratrol by inhibiting oxidative damage and nuclear factor-κB activation. Investig. Ophthalmol. Vis. Sci. 50, 3512–3519. https://doi.org/10.1167/iovs.08-2666.

Li, A.N., Li, S., Zhang, Y.J., Xu, X.R., Chen, Y.M., Li, H.B., 2014. Resources and biological activities of natural polyphenols. Nutrients 6, 6020–6047. https://doi.org/10.3390/nu6126020.

Li, M., Zhang, L., Li, R., Yan, M., 2020. New resveratrol micelle formulation for ocular delivery: characterization and in vitro/in vivo evaluation. Drug Dev. Ind. Pharm. 46, 1960–1970. https://doi.org/10.1080/03639045.2020.1828909.

Loftsson, T., Brewster, M.E., 2012. Cyclodextrins as functional excipients: methods to enhance complexation efficiency. J. Pharm. Sci. 101, 2271–2280. https://doi.org/10.1002/jps.

Loftsson, T., Duchêne, D., 2007. Cyclodextrins and their pharmaceutical applications. Int. J. Pharm. 329, 1–11. https://doi.org/10.1016/j.ijpharm.2006.10.044.

Loftsson, T., Hreinsdóttir, D., Másson, M., 2005. Evaluation of cyclodextrin solubilization of drugs. Int. J. Pharm. 302, 18–28. https://doi.org/10.1016/j.ijpharm.2005.05.042.

Loftsson, T., Stefánsson, E., 1997. Effect of cyclodextrins on topical drug delivery to the eye. Drug Dev. Ind. Pharm. 23, 473–481. https://doi.org/10.3109/03639049709148496.

Lollett, I.V., Galor, A., 2018. Dry eye syndrome: Developments and lifitegrast in perspective. Clin. Ophthalmol. 12, 125–139. https://doi.org/10.2147/OPTH.S126668.

Messner, M., Kurkov, S.V., Jansook, P., Loftsson, T., 2010. Self-assembled cyclodextrin aggregates and nanoparticles. Int. J. Pharm. 387, 199–208. https://doi.org/10.1016/j.ijpharm.2009.11.035.

Nita, M., Grzybowski, A., 2016. The Role of the Reactive Oxygen Species and Oxidative Stress in the Pathomechanism of the Age-Related Ocular Diseases and Other Pathologies of the Anterior and Posterior Eye Segments in Adults. Oxid. Med. Cell. Longev. 2016, 1–23.

Robinson, K., 2015. Pre-formulation studies of resveratrol. Drug Dev. Ind. Pharm. 41, 1464–1469. https://doi.org/10.3109/03639045.2014.958753.Pre-formulation.

Salehi, B., Mishra, A.P., Nigam, M., Sener, B., Kilic, M., Sharifi-Rad, M., Fokou, P.V.T., Martins, N., Sharifi-Rad, J., 2018. Resveratrol: A double-edged sword in health benefits. Biomedicines 6, 1–20. https://doi.org/10.3390/biomedicines6030091.

Saokham, P., Muankaew, C., Jansook, P., Loftsson, T., 2018. Solubility of cyclodextrins and drug/cyclodextrin complexes. Molecules 23, 1–15. https://doi.org/10.3390/molecules23051161.

Seen, S., Tong, L., 2018. Dry eye disease and oxidative stress. Acta Ophthalmol. 96, e412–e420. https://doi.org/10.1111/aos.13526.

Snetkov, P., Zakharova, K., Morozkina, S., Olekhnovich, R., Uspenskaya, M., 2020. Hyaluronic acid: The influence of molecular weight on structural, physical, physico-chemical, and degradable properties of biopolymer. Polymers (Basel). 12 (8), 1800.

Sokolová, R., Degano, I., Ramešová, Š., Bulíčková, J., Hromadová, M., Gál, M., Fiedler, J., Valášek, M., 2011. The oxidation mechanism of the antioxidant quercetin in nonaqueous media. Electrochim. Acta 56, 7421–7427. https://doi.org/10.1016/j.electacta.2011.04.121.

Uchino, Y., Kawakita, T., Miyazawa, M., Ishii, T., Onouchi, H., Yasuda, K., Ogawa, Y., Shimmura, S., Ishii, N., Tsubota, K., Einwaechter, H., 2012. Oxidative Stress Induced Inflammation Initiates Functional Decline of Tear Production. PLoS One 7 (10), e45805.

Vizzarri, F., Palazzo, M., Bartollino, S., Casamassima, D., Parolini, B., Troiano, P., Caruso, C., Costagliola, C., 2018. Effects of an antioxidant protective topical formulation on eye exposed to ultraviolet-irradiation: A study in rabbit animal model. Physiol. Res. 67, 457–464. https://doi.org/10.33549/physiolres.933759.

Wang, J., Zhao, Xi.H., 2016. Degradation kinetics of fisetin and quercetin in solutions affected by medium pH, temperature and co-existing proteins. J. Serbian Chem. Soc. 81, 243–253. https://doi.org/10.2298/JSC150706092W.

Wang, W., Sun, C., Mao, L., Ma, P., Liu, F., Yang, J., Gao, Y., 2016. The biological activities, chemical stability, metabolism and delivery systems of quercetin: A review. Trends Food Sci. Technol. 56, 21–38. https://doi.org/10.1016/j.tifs.2016.07.004.

Yamaguchi, T., 2018. Inflammatory response in dry eye. Investig. Ophthalmol. Vis. Sci. 59, DES192–DES199. https://doi.org/10.1167/iovs.17-23651.

Yang, S., Lian, G., 2020. ROS and diseases: role in metabolism and energy supply. Mol. Cell. Biochem. 467, 1–12. https://doi.org/10.1007/s11010-019-03667-9.

Zhao, L., Wang, H., Du, X., 2021. The therapeutic use of quercetin in ophthalmology: recent applications. Biomed. Pharmacother. 137, 111371 https://doi.org/10.1016/j.biopha.2021.111371.

Zupančič, Š., Lavrič, Z., Kristl, J., 2015. Stability and solubility of trans-resveratrol are strongly influenced by pH and temperature. Eur. J. Pharm. Biopharm. 93, 196–204. https://doi.org/10.1016/j.ejpb.2015.04.002.